Polymer 51 (2010) 6182–6192

Contents lists available at ScienceDirect

Polymer

journal homepage: www.elsevier.com/locate/polymer

# Synthesis and application of H-Bonded cross-linking polymers containing a conjugated pyridyl H-Acceptor side-chain polymer and various carbazole-based H-Donor dyes bearing symmetrical cyanoacrylic acids for organic solar cells

Duryodhan Sahu [a], Harihara Padhy [a], Dhananjaya Patra [a], Dhananjay Kekuda [b], Chih-Wei Chu [b,c], I-Hung Chiang [a], Hong-Cheu Lin [a,*]

[a] Department of Materials Science and Engineering, National Chiao Tung University, Hsinchu, Taiwan, ROC
[b] Research Center for Applied Sciences, Academia Sinica, Taipei, Taiwan, ROC
[c] Department of Photonics, National Chiao Tung University, Hsinchu, Taiwan, ROC

ARTICLE INFO

*Article history:*
Received 12 August 2010
Received in revised form
4 October 2010
Accepted 10 October 2010
Available online 26 October 2010

*Keywords:*
H-bonded polymer network
Solar cell
Self-assembly

ABSTRACT

A series of novel hydrogen-bonded (H-bonded) cross-linking polymers were generated by complexing various proton-donor (H-donor) solar cell dyes containing 3,6- and 2,7-functionalized electron-donating carbazole cores bearing symmetrical thiophene linkers and cyanoacrylic acid termini with a proton-acceptor (H-acceptor) side-chain homopolymer carrying pyridyl pendants (with 1/2 M ratio of H-donor/H-acceptor). The supramolecular H-bonded structures between H-donor dyes and the H-acceptor side-chain polymer were confirmed by FTIR measurements. The effects of the supramolecular architecture on optical, electrochemical, and organic photovoltaic (OPV) properties were investigated. From DFT (density functional theory) calculations, the optimized geometries of organic dyes reflected that the carbazole cores of H-donor dyes were coplanar with the conjugated thiophenes and cyanoacrylic acids, which is essential for strong conjugations across the donor-acceptor units in **D1**–**D4** dyes. Under 100 mW/cm$^2$ of AM 1.5 white-light illumination, bulk heterojunction (BHJ) OPV cell devices containing an active layer of H-bonded polymers (**PDFTP/D1**–**D4**) as an electron donor blended with [6,6]-phenyl $C_{61}$-butyric acid methyl ester (PCBM) as an electron acceptor in a weight ratio of 1:1 were explored. From the preliminary investigations, the OPV device containing 1:1 weight ratio of H-bonded polymer **PDFTP/D2** and PCBM showed the best power conversion efficiency (PCE) value of 0.31% with a short-circuit current ($J_{sc}$) of 1.9 mA/cm$^2$, an open-circuit voltage ($V_{oc}$) of 0.55 V, and a fill factor (FF) of 29%, which has a higher PCE value than the corresponding H-donor **D2** dye (PCE = 0.15%) or H-acceptor **PDFTP** homopolymer (PCE = 0.02%) blended with PCBM in 1:1 weight ratio.



## 1. Introduction

In order to overcome the growing global energy needs, extensive researches on environment friendly and renewable sources of energies have been made during the past decade [1,2]. As an ecologically sustainable and renewable source of energies, solar energy led to a greater attention for the scientists to develop solar energy conversion devices [3,4]. Since then, π-conjugated oligomers and polymers were applied as advanced materials for the development of organic photovoltaic (OPV) devices for future applications [5,6]. After the breakthrough work of Heeger and coworkers in 1995 [7], bulk heterojunction (BHJ) solar cells became a low-cost, flexible, and large-area processible [8,9] alternatives to silicon-based solar cells, though their efficiencies are not comparable to those of silicon-based technologies. In fact, different solar cell architectures have been developed, including dye sensitized solar cells [10–12], donor-acceptor BHJs of polymer blends [13–19] and block copolymers [20], supramolecular ensemble of small molecule/small molecule [21] etc. However, the interests on oligomers with easy purification processes and lack of problems in molecular weight distributions etc. are generally auxiliary to their polymer analogues due to the better solvent processabilities and film morphologies in photovoltaic cells [22]. Therefore, in order to get the advantages of both oligomeric and polymeric properties, an attractive approach would be the well-defined supramolecular architectures of π-conjugated oligomers with the processabilities of polymers [23].

Since conjugated polymers with electron donor-acceptor (D-A) architectures had proved as the highly efficient solar cell polymers

* Corresponding author. Tel.: +8863 5712121x55305; fax: +8863 5724727.
*E-mail address:* linhc@cc.nctu.edu.tw (H.-C. Lin).

0032-3861/$ – see front matter © 2010 Elsevier Ltd. All rights reserved.
doi:10.1016/j.polymer.2010.10.018

that built intramolecular charge transfer (ICT) transitions from the electron donor to acceptor and thus to lower the band gaps of solar cell polymers [24]. Carbazole-based oligomers and polymers as semiconducting materials have been attracted attentions for its good chemical stability, easy functionalization with a large variety of substituents to modulate the carbazole properties without increasing the steric hindrance, and cheap availabilities of starting materials towards organic materials applications of organic light-emitting diodes (OLEDs) [25], organic field effect transisters (OFETs) [26] and organic photovoltaics (OPVs) [27]. The electron rich nitrogen and sulphur atoms in carbazole and thiophene units respectively enhance their potentials as efficient p-type transporting moieties in those applications. After the successful synthesis of N-alkyl-2,7-diiodocarbazole by Leclerc at.el [28], 2,7-functionalized carbazole became the promising candidate with more planar and well delocalized π-electron structure for the applications of organic photovoltaics [29]. There are many reports of carbazole-based polymers or oligomers in the field of bulk heterojunction (BHJ) organic photovoltaics (OPVs) [30]. However, in order to get high power conversion efficiency (PCE) values, self-assembles of π-conjugated oligomers with processable polymers into well-defined and organized D-A supramolecular structures remain a challenge [23]. Previously, Meijer and coworkers employed a supramolecular H-bonded polymer containing oligo(p-phenylene vinyene) and ureido-pyrimidinone units (as H-bonded groups) for the applications in OPV devices [22a,31]. Furthermore, we reported on supramolecular assemblies of H-bonded side-chain polymers which were prepared by complexation of light-emitting dendrimers or solar cell dyes bearing carboxylic acids as proton-donors (H-donors) with side-chain polymers bearing pyridyl pendants as proton-acceptors (H-acceptors) for the applications in OLEDs and OPVs [32]. In general, different attempts of utilizing conjugated oligomers/polymers or both have been made to design electron donor-acceptor architectures to enhance the intramolecular charge transfer interactions from the electron donors to the electron acceptors and thus to increase the PCE values.

As shown in Fig. 1, a series of symmetrical carbazole-based conjugated dyes (**D1**–**D4**) containing carbazole cores functionalized at two different (i.e., 3,6- and 2,7-substituted) positions linked to cyanoacrylic acid termini (as double H-donors) via π-conjugated oligo-thiophenes were synthesized, which were complexed with a side-chain homopolymer (**PDFTP**) bearing pyridyl pendants (as H-acceptors). Then, double H-donors of **D1**–**D4** dyes and H-acceptors of side-chain homopolymer **PDFTP** can be self-assembled into H-bonded cross-linking polymers, and the schematic illustration is demonstrated in Fig. 2. The supramolecular (H-bonded) polymer networks (**PDFTP/D1**–**D4**) of carbazole-based H-donor dyes (**D1**–**D4**) complexed with side-chain H-acceptor homopolymer (**PDFTP**) were confirmed by FTIR spectroscope. The active layer of blended polymers of H-bonded polymer networks **PDFTP/D1**–**D4** as electron donors and (6,6)-phenyl $C_{61}$-butyric acid methyl ester (PCBM) as an electron acceptor (in a weight ratio of 1:1) were subjected to BHJ photovoltaic investigations (under AM 1.5 irradiation, 100 mW/cm$^2$). From the preliminary results, the solar cell device containing H-bonded polymer network **PDFTP/D2** produced the best PCE value of 0.31%, which was obviously doubled the PCE value (0.15%) of the active layer of **D2** dye alone blended with PCBM, fabricated and measured under similar conditions.

## 2. Experimental

### 2.1. Materials

Chemicals and solvents were reagent grades and purchased from Aldrich, ACROS, TCI, Strem, Fluka, and Lancaster Chemical Co. THF and dichloromethane were distilled over sodium/benzophenone and calcium hydride respectively and freshly distilled before

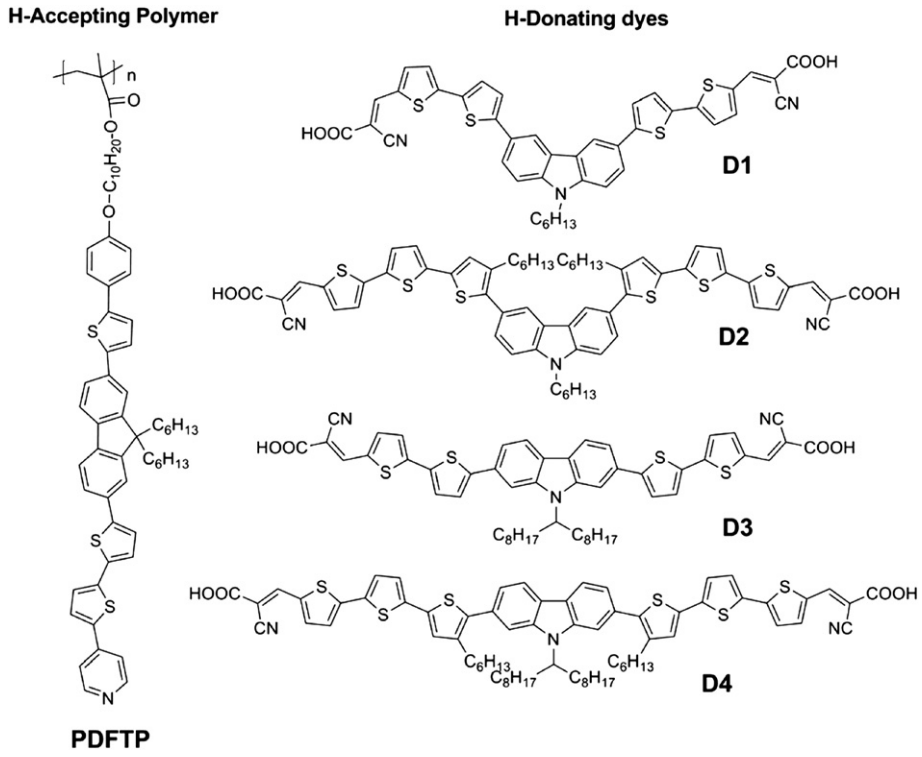


**Fig. 1.** Structures of H-acceptor side-chain polymer (**PDFTP**) and H-donor dyes (**D1**–**D4**) used in supramolecular (H-bonded) cross-linking polymers.

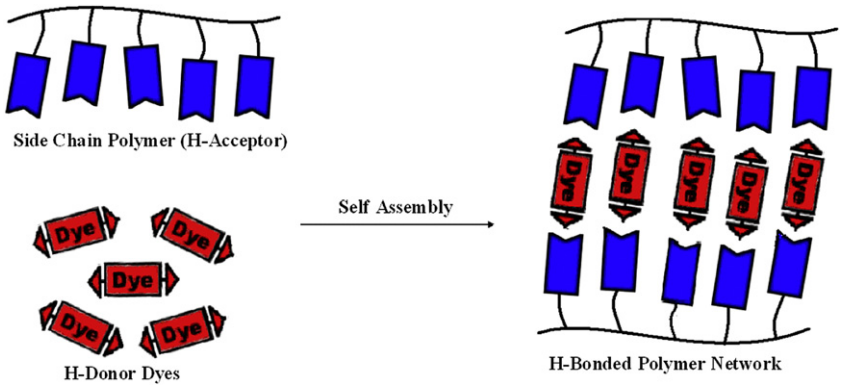


**Fig. 2.** Schematic illustration of H-bonded polymer networks (**PDFTP/D1**–**D4**) containing H-donor dyes (**D1**–**D4**) and H-acceptor side-chain polymer (**PDFTP**).

use. Tetra-n-butyl ammonium hexafluorophosphate ($TBAPF_6$) was recrystallized twice from absolute ethanol and further dried for two days under vacuum. N-bromosuccinimide was recrystallized from distilled water and dried under vacuum. The other chemicals were used without further purification. Chromatography was performed with Merck silica gel (mesh 70–230) and basic aluminum oxide, deactivated with water. The chemical structures for all products were confirmed by $^1$H NMR spectroscopy, mass spectra (FAB) and elemental analyses.

### 2.2. Measurements

$^1$H NMR spectra were recorded on a Varian unity 300 MHz spectrometer using *d*-DMSO as solvents. Elemental analyses were performed on a HERAEUS CHN-OS RAPID elemental analyzer. Fourier transform infrared (FT-IR) spectra were performed a Nicolet 360 FT-IR spectrometer. Thermo gravimetric analyses (TGA) were conducted on a Du Pont Thermal Analyst 2100 system with a TGA 2950 thermo gravimetric analyzer at a heating rate of 20 °C/min under nitrogen. Gel permeation chromatography (GPC) analyses were conducted with a Water 1515 separations module using polystyrene as a standard and THF as an eluent. UV–visible absorption spectra were recorded in dilute THF solutions ($10^{-5}$ M) on an HP G1103A spectrophotometer. Fourier transform infrared (FTIR) spectra of samples dispersed in KBr disks were recorded on a Perkin–Elmer Spectrum 100 Series [32a].

Thin films of UV–vis were spin-coated on quartz substrates from THF solutions with a concentration of 1 wt%. Cyclic voltammetry (CV) measurements were performed using a BAS 100 electrochemical analyzer with a standard three-electrode electrochemical cell in a 0.1 M tetrabutylammonium hexafluorophosphate ($TBAPF_6$) solution at room temperature with a scanning rate of 100 mV/s. During the CV measurements, the solutions were purged with nitrogen for 30 s. In H-bonded cross-linking polymers, a carbon working electrode coated with a thin layer of H-bonded polymer, and for dyes in solution (THF) a platinum wire as the counter electrode, and a silver wire as the quasi-reference electrode were used, and Ag/AgCl (3 M KCl) electrode was served as a reference electrode for all potentials quoted herein. The redox couple of ferrocene/ferrocenium ion ($Fc/Fc^+$) was used as an external standard. The corresponding highest occupied molecular orbital (HOMO) and lowest unoccupied molecular orbital (LUMO) levels were calculated using $E_{ox/onset}$ and $E_{red/onset}$. The onset potentials were determined from the intersections of two tangents drawn at the rising currents and background currents of the cyclic voltammetry (CV) measurements.

### 2.3. Quantum chemistry computation

The predicted structures of the molecules were optimized by using B3LYP hybrid functional [33] and 6-31G* basis sets [34]. For each of the molecules, a number of conformational isomers were examined and the one with the lowest energy was used. All of the analyses were performed under Gaussian 03 (G03) (revision E.01) program package [35] by using density functional theory (DFT).

### 2.4. Fabrication and characterization of OPV devices

Solar cells were fabricated on indium tin oxide (ITO)-coated glass substrates through a following procedure: The ITO coated glass substrate was first cleaned with a detergent and sonicated in an ultrasonic bath, and they were dried overnight in an oven. After this cleaning procedure, the substrates were subjected to UV ozone cleaning for 15 min. PEDOT: PSS (Baytron PH) was spin coated onto the substrates at 4000 rpm. The films were dried on a hotplate at 120 °C for 30 min. The samples were then transferred to the nitrogen filled glove box for the active layer deposition. A solution containing hydrogen-bonded polymer networks (**PDFTP/Dx**, where **x** vary from 1 to 4) and PCBM were prepared (2 wt%, 1:1) and were kept overnight digitally controlled hotplate at 60 °C for the uniform mixing. The solutions were used for the active layer deposition and were spin coated on the substrates at 1500 rpm for 60 s. The films were allowed to dry in a covered Petri dish. No thermal annealing treatment was given to the active layers prior to the cathode deposition. Finally, a 20 nm Ca and 50 nm Al cathodes were deposited using a thermal evaporator at a base pressure of $1 \times 10^{-6}$ Torr. The device area was 0.1 $cm^2$. The devices were then transferred to the nitrogen filled glove box. The current-voltage characteristics of the devices were measured using HP 4156 semiconductor parameter analyzer. Air mass 1.5 Global (AM 1.5 G) solar simulator was used for the photo illumination of the devices.

### 2.5. Synthesis of monomer and dyes

Carbazole-based donor dyes **D1**–**D4** (as shown in Fig. 1) were synthesized from 9-hexyl-3,6-bis(4,4,5,5-tetramethyl-1,3,2-dioxaborolan-2-yl)-9H-carbazole(**D1**–**D2**) [36] and 9-(heptadecan-9-yl)-2,7-bis(4,4,5,5-tetramethyl-1,3,2-dioxaborolan-2-yl)-9H-carbazole (**D3**–**D4**) [37]. Intermediates **7**–**10** were synthesized by the similar Suzuki coupling conditions, and one of the synthetic procedures (for intermediate **7**) has been described. The monomers **D1**–**D4** were acquired from the previous intermediates via Knoevenagel condensation reaction. Their synthetic routes are shown in Scheme S1 and detailed procedures for intermediates are described in the

supporting information. Monomer **DFTP** was synthesized from 2,7, dibromofluorene as a starting material and polymerized with free radical polymerization using AIBN as an initiator are shown in Scheme 1. The $^1$H NMRs of the monomer **DFTP** and side-chain homopolymer (**PDFTP**) are shown in Fig. 3 and the detailed procedures for monomer **DFTP** and homopolymer **PDFTP** are described as follows:

*2.5.1. 2,7-Dibromo-9,9-dihexyl-9H-fluorene (**1**)*

A mixture of 2,7-dibromofluorene (10 g, 30.86 mmol) and potassium-tert-butoxide (10.37 g, 92.58 mmol) were stirred in 120 ml of dry THF under nitrogen for 1 h, then 1-bromohexane (11 ml, 78.00 mmol) was added drop wise and refluxed for overnight. Excess of THF was removed by rotary evaporator. Next, the compound was extracted with dichloromethane and washed with water followed by a little brine. Then, the organic layer was dried over anhydrous $MgSO_4$ (worked up). The solvent was removed by rotary evaporator, and the crude product was purified by column chromatography (silica) using hexane as an eluent to yield a white solid (13.40 g, 88%). $^1$H NMR (300 MHz, $CDCl_3$), $\delta$ (ppm): 7.50 (s, 2H), 7.46 (d, $J$ = 1.5 Hz, 2H), 7.44 (d, $J$ = 1.8 Hz, 2H), 1.93–1.88 (m, 4H), 1.17 (m, 4H), 1.13–1.03 (m, 12H), 0.78 (t, $J$ = 6.9 Hz, 6H).

*2.5.2. 2,2′-(9,9-Dihexyl-9H-fluorene-2,7-diyl)dithiophene (**2**)*

Compound **1** (5 g, 10.15 mmol), thiophen-2-ylboronic acid (3.3 g, 25.78 mmol), $K_2CO_3$ (4.2 g, 30.40 mmol) were reacted in 300 ml of toluene and ethanol (3:1) and degassed for 10 min then $Pd(PPh_3)_4$ (293 mg, 0.253 mmol) was added and then the resulting mixture was stirred under reflux for 4 h. The reaction mixture was worked

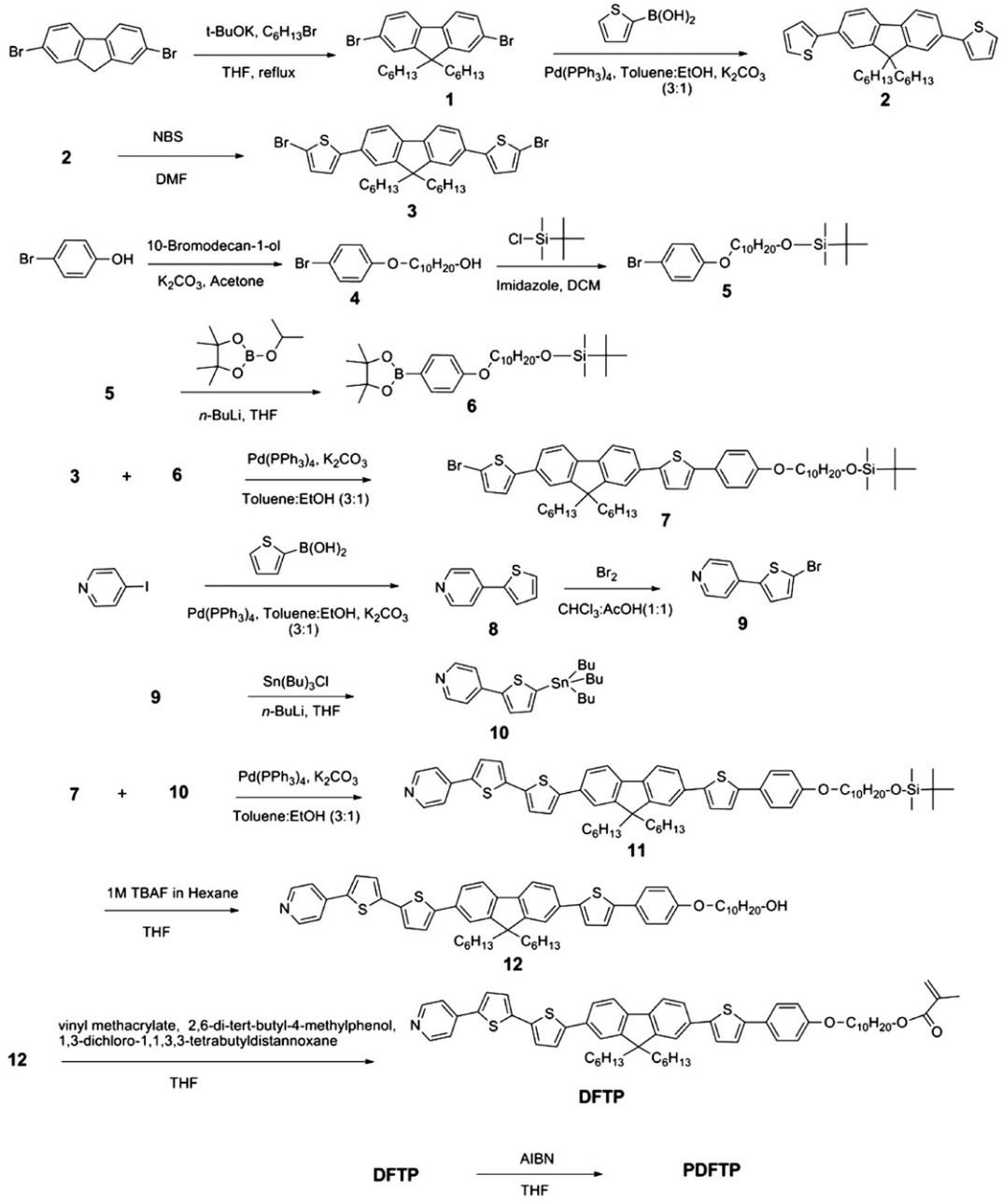


**Scheme 1.** Synthetic route of H-acceptor side-chain polymer (**PDFTP**).

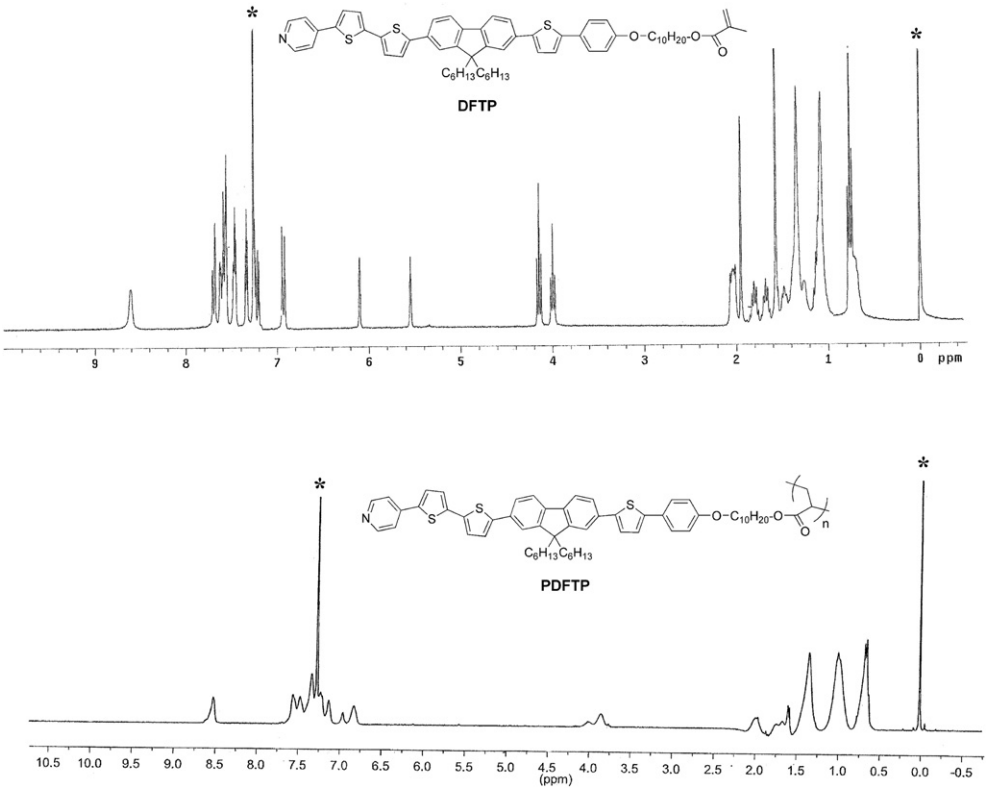


**Fig. 3.** $^1$H NMR spectra of monomer **DFTP** and H-acceptor polymer **PDFTP** in $CDCl_3$. (* indicates the solvent peak).

up, then the excess solvent was concentrated under vacuum. Subsequently, the compound was purified by column chromatography (silica) using hexane as an eluent to yield a white solid (4.8 g, 96%). $^1$H NMR (300 MHz, $CDCl_3$), $\delta$(ppm): 7.69 (d, $J$ = 7.8 Hz, 2H), 7.63–7.57 (m, 4H) 7.40 (d, $J$ = 3 Hz, 2H), 7.30 (d, $J$ = 5.2 Hz, 2H), 7.13–7.10 (m, 2H), 2.05–2.00 (m, 4H), 1.14–1.06 (m, 12H), 0.78–0.69 (m, 10H).

### 2.5.3. 5,5′-(9,9-Dihexyl-9H-fluorene-2,7-diyl)bis(2-bromothiophene) (**3**)

Compound **2** (5 g, 10 mmol) was dissolved in 120 ml of DMF, to that N-bromosuccinimide (4.1 g, 23.05 mmol, freshly purified by recrystallization from water) was added portion wise and stirred for overnight at room temperature, sequentially. The reaction mixture was worked up and the solvent was removed under vacuum. Then, the compound was purified by column chromatography (silica) using hexane as an eluent to yield a white solid (6.1 g, 93%). $^1$H NMR (300 MHz, $CDCl_3$), $\delta$(ppm): 7.66 (d, $J$ = 7.8 Hz, 2H), 7.50 (d, $J$ = 1.5 Hz, 1H) 7.48 (d, $J$ = 1.5 Hz, 1H), 7.45 (d, $J$ = 1.5 Hz, 2H), 7.11 (d, $J$ = 3.9 Hz, 2H), 7.05 (d, $J$ = 3.9 Hz, 2H), 2.01–1.96 (m, 4H), 1.14–1.04 (m, 12H), 0.77–0.63(m, 10H).

### 2.5.4. 10-(4-Bromo-phenoxy)-decanol (**4**)

4-Bromophenol (10 g, 57.8 mmol), 10-bromo decanol (16.45 g, 69.36 mmol), and $K_2CO_3$ (23.96 g, 173.33 mmol) was dissolved in 150 ml of dry acetone and stirred under reflux for 24 h. After cooling to room temperature, the potassium salt was filtered off and the solvent was removed by rotary evaporator followed by similar work up procedure, then the excess solvent was removed using rotary evaporator. The crude product was purified by column chromatography (silica) using mixture of hexane and ethyl acetate (4:1) as an eluent, to get low melting semi solid (15.2 g, 80%).$^1$H NMR (300 MHz, $CDCl_3$), $\delta$ (ppm): 7.33 (d, $J$ = 9.0 Hz, 2H), 6.75 (d, $J$ = 9.0 Hz, 2H), 3.89 (t, $J$ = 6.3 Hz, 2H), 3.62 (t, $J$ = 6.6 Hz, 2H), 1.78–1.69 (m, 2H), 1.59–1.50 (m, 2H), 1.41–1.29 (m, 12H).

### 2.5.5. [10-(4-Bromo-phenyl)-decyloxy]-tert-butyl-dimethyl-silane (**5**)

Mixture of compound **4** (5 g, 15.18 mmol) and imidazole (2.00 g, 30.30 mmol) were dissolved in 100 ml of dry dichloromethane and degassed for 10 min. Tert-butyl-chloro-dimethyl-silane (4.57 g, 30.30 mmol) was added at 0 °C under nitrogen atmosphere and stirred further to react for 4 h at room temperature, then the reacting mixture was worked up and the excess solvent was removed using rotary evaporator. Subsequently, the crude product was purified by column chromatography (silica) using mixture of hexane and dichloromethane (4:1) as eluent, to get a colorless liquid (5.5 g, 82%).$^1$H NMR (300 MHz, $CDCl_3$), $\delta$ (ppm): 7.34 (d, $J$ = 12 Hz, 2H), 6.76 (d, $J$ = 8.1 Hz, 2H), 3.90 (t, $J$ = 15 Hz, 2H) 3.60 (t, $J$ = 15 Hz, 2H), 1.73(m, 2H), 1.30–1.51 (m, 14H), 0.89 (s, 9H), 0.05 (s, 6H).

### 2.5.6. 2-{4-[10-(Tert-butyl-dimethyl-silanyloxy)-decyl]-phenyl}-4,4,5,5-tetramethyl-[1,3,2] dioxaborolane (**6**)

5 g of compound **5** (11.27 mmol) was dissolved in 100 ml of dry THF and the solution was cooled to − 78 °C under nitrogen atmosphere then 9 ml of *n*-BuLi (2.5 M in hexane, 22.54 mmol) was added. The solution was warmed up to room temperature and stirred for 2 h and cooled again to − 78 °C, then 6.13 ml (22.54 mmol) of 2-Isopropoxy-4,4,5,5-tetramethyl- [1,3,2] dioxaborolane was injected promptly in to the flask and the resulting mixture was stirred overnight at room temperature. The reaction was quenched by adding 50 ml of water then extracted with dichloromethane, and a little of brine. Thereafter the organic solvent was dried over anhydrous $MgSO_4$ and the solvent was removed by rotary evaporator. The crude product was purified by

column chromatography (silica) using mixture of hexane and dichloromethane (4:1) as eluent to yield a low melting white solid (3.5 g, 63%). $^1$H NMR (300 MHz, $CDCl_3$), $\delta$ (ppm): 7.72 (d, $J$ = 8.4 Hz, 2H), 6.87(d, $J$ = 8.7 Hz, 2H), 3.95(t, $J$ = 12.9 Hz, 2H), 3.57(t, $J$ = 13.5 Hz, 2H), 1.73(qn, $J$ = 6.9 Hz, 2H), 1.54–1.22 (m, 26H), 0.86 (s, 9H), 0.02 (s, 6H).

*2.5.7. (10-(4-(5-(7-(5-Bromothiophen-2-yl)-9,9-dihexyl-9H-fluoren-2-yl)thiophen-2-yl)phenoxy)decyloxy) (tert-butyl) dimethylsilane (**7**)*

Mixture of compound **3** (3 g, 4.56 mmol), **6** (1.9 g, 3.9 mmol), and $K_2CO_3$ (0.7 g, 5.03 mmol) were dissolved in 80 ml of toluene and ethanol (3:1) and degassed for 10 min. Then $Pd(PPh_3)_4$ (115 mg, 0.10 mmol) was added and the resulting mixture was stirred under reflux for overnight. The solvent was removed under vacuum, and after being worked up the solvent was concentrated by rotary evaporator. Then, the compound was purified by column chromatography (silica) using a mixture of hexane and dichloromethane (9:1) as an eluent, to get a yellow solid (2.00 g, 55%) $^1$H NMR (300 MHz, $CDCl_3$), $\delta$(ppm): 7.66 (d, $J$ = 7.8 Hz, 2H), 7.59–7.53(m, 5H) 0.7.36 (dd, $J$ = 3.6 Hz, $J$ = 1.2 Hz, 1H), 7.31 (d, $J$ = 3.9 Hz, 1H), 7.27 (dd, $J$ = 5.1 Hz, $J$ = 1.2 Hz, 1H), 7.18 (d, $J$ = 3.9 Hz, 1H), 7.10–7.08 (m, 1H), 6.90 (d, $J$ = 9 Hz, 2H), 3.97 (t, $J$ = 6.6 Hz, 2H), 3.58(t, $J$ = 13.5 Hz, 2H), 2.03–1.97 (m, 4H), 1.83–1.76 (m, 2H), 1.51–1.25 (m, 16H), 1.13–1.05 (m, 10H), 0.88 (s, 9H), 0.75–0.67 (m, 10H), 0.035 (s, 6H).

*2.5.8. 4-(Thiophen-2-yl) pyridine (**8**)*

Mixture of compound 4-iodopyridine (2 g, 9.75 mmol), thiophen-2-ylboronic acid (1.5 g, 11.7 mmol), $K_2CO_3$ (1.8 g, 13 mmol) were dissolved in 120 ml of toluene and ethanol (3:1) and degassed for 10 min then $Pd(PPh_3)_4$ (225 mg, 0.195 mmol) was added and then the resulting mixture was stirred under reflux for overnight. The solvent was removed under vacuum followed by work up procedure, then the solvent was concentrated under vacuum. Thereafter, the compound was purified by column chromatography ($Al_2O_3$) using mixture of hexane and dichloromethane (9:1) as eluent, to get a white solid (1.4 g, 86%) $^1$H NMR (300 MHz, $CDCl_3$), $\delta$ (ppm): 8.57 (d, $J$ = 6 Hz, 2H), 7.50–7.46 (m, 3H), 7.40 (d, $J$ = 5.1 Hz, 1H), 7.12 (t, $J$ = 4.2 Hz, 1H).

*2.5.9. 4-(5-Bromothiophen-2-yl) pyridine (**9**)*

4-(thiophen-2-yl)pyridine (**8**) (1 g, 6.2 mmol) was dissolved in 50 ml of dichloromethane, to that, bromine (0.63 ml, 12.4 mmol) with 10 ml of dichloromethane was added slowly for 10 min and stirred for additional 15 min at room temperature. The reaction was quenched with 50 ml of 10% $K_2CO_3$ followed by extraction from dichloromethane and dried over anhydrous $MgSO_4$. Subsequently, the solvent was concentrated by rotary evaporator. After that, the compound was purified by column chromatography on $Al_2O_3$ using mixture of hexane and dichloromethane (10:1) as eluent, to get white solid (1.2 g, 81%) $^1$H NMR (300 MHz, $CDCl_3$), $\delta$(ppm): 8.60 (d, $J$ = 6 Hz, 2H), 7.45 (d, $J$ = 6 Hz, 2H), 7.30 (d, $J$ = 3 Hz, 1H), 7.11 (d, $J$ = 3 Hz, 1H).

*2.5.10. 2-Tri-n-butylstannyl-5-(4-pyridyl) thiophene (**10**)*

4-(5-bromothiophen-2-yl) pyridine (**9**) (0.3 g, 1.24 mmol) was dissolved in 80 ml of THF and the solution was cooled to - 78 °C. 0.75 ml (2.5 M in hexane, 1.87 mmol) of *n*-BuLi was added over a period of 3 min under nitrogen atmosphere. After stirring the solution for 30 min at - 78 °C, $Bu_3SnCl$ (0.5 ml, 1.87 mmol) was added and the reaction mixture was stirred for further 1 h. It was then allowed to warm up to room temperature and stirred for additional 3 h then the reaction was quenched with water (30 ml). THF was removed in rotary evaporator and worked up, then the solvent was removed in rotary evaporator. Afterward, the compound was purified by column chromatography($Al_2O_3$) using a mixture of hexane and ethyl acetate (5:1) as eluent, to get a yellow oil (0.45 g, 80%) $^1$H NMR (300 MHz, $CDCl_3$), $\delta$(ppm): 8.56 (d, $J$ = 4.8 Hz, 2H), 7.60 (d, $J$ = 3.3 Hz, 1H), 7.48 (d, $J$ = 6.3 Hz, 2H), 7.19 (d, $J$ = 3.3 Hz, 1H), 1.64–1.53 (m, 6H), 1.39–1.26 (m, 6H), 1.17–1.11 (m, 6H), 0.90 (t, $J$ = 7.5 Hz, 9H).

*2.5.11. 4-(5′-(7-(5-(4-(10-(tert-Butyldimethylsilyloxy)decyloxy) phenyl)thiophen-2-yl)-9,9-dihexyl-9H-fluoren-2-yl)-2,2′-bithiophen-5-yl)pyridine (**11**)*

Mixture of compound **7** (2 g, 2.12 mmol), compound **10** (1 g, 2.22 mmol) and $Pd(PPh_3)_4$ (0.3 g, 0.26 mmol) were added to toluene (200 ml) and degassed for 10 min. Then the mixture was heated to reflux for 24 h under nitrogen atmosphere. The solvent was removed under vacuum. After the similar work up procedure, the solvent was concentrated by rotary evaporator, and then the compound was purified by column chromatography ($Al_2O_3$) using dichloromethane as eluent, to get a yellow solid (1.3 g, 60%) $^1$H NMR (300 MHz, $CDCl_3$), $\delta$(ppm): 8.57 (d, $J$ = 6.3 Hz, 2H), 7.70 (d, $J$ = 3 Hz, 1H), 7.67 (d, $J$ = 3 Hz, 1H), 7.62–7.50(m, 10H), 7.32 (d, $J$ = 3.6 Hz, 2H), 7.25 (d, $J$ = 5.7 Hz, 1H), 7.18 (d, $J$ = 3.9 Hz, 1H), 6.90 (d, $J$ = 9 Hz, 2H), 3.96 (t, $J$ = 6.9 Hz, 2H), 3.58 (t, $J$ = 6.6 Hz, 2H), 2.13–2.05 (m, 4H), 1.80–1.76 (m, 2H), 1.49–1.28 (m, 16H), 1.11–1.05 (m, 10H), 0.88 (s, 9H), 0.75–0.67 (m, 10H), 0.042 (s, 6H).

*2.5.12. 10-(4-(5-(9,9-Dihexyl-7-(5′-(pyridin-4-yl)-2,2′-bithiophen-5-yl)-9H-fluoren-2-yl)thiophen-2-yl)phenoxy)decan-1-ol (**12**)*

Compound **11** (0.9 g, 0.88 mmol) was dissolved in 30 ml of dry THF, to this 1.75 ml (1.76 mmol) of 1M TBAF was added under an ice-cold water bath. The reaction mixture was stirred for 10 min then further 12 h at room temperature. THF was removed by rotary evaporator, the product was extracted with excess of dichloromethane followed by brine wash .The organic solvent was dried over anhydrous magnesium sulphate then the solvent was removed using rotary evaporator. The crude product was purified by column chromatography on $Al_2O_3$ using mixture of dichloromethane:THF (20:1) as an eluent to yield a yellow solid (0.65 g, 81%) $^1$H NMR (300 MHz, $CDCl_3$), $\delta$(ppm): 8.70 (d, $J$ = 5.4 Hz, 2H), 8.05 (d, $J$ = 3.9 Hz, 2H), 7.96 (d, $J$ = 6.3 Hz, 2H), 7.82–7.73 (m, 4H), 7.66–7.54 (m, 7H), 7.40 (d, $J$ = 3.6 Hz, 1H), 6.95 (d, $J$ = 8.7 Hz, 2H), 3.99 (t, $J$ = 6.6 Hz, 2H), 3.64 (t, $J$ = 6.6 Hz, 2H), 2.06–2.01 (m, 4H), 1.82–1.77 (m, 2H), 1.59–1.53 (m, 2H), 1.47–1.43 (m, 14H), 1.15–1.07 (m, 10H), 0.77–0.72 (m, 10H).

*2.5.13. 10-(4-(5-(9,9-Dihexyl-7-(5′-(pyridin-4-yl)-2,2′-bithiophen-5-yl)-9H-fluoren-2-yl)thiophen-2-yl)phenoxy)decyl methacrylate (DFTP)*

To a schlenk tube, compound **12** (1.0 g, 1.10 mmol), vinyl methacrylate (0.37 g, 3.3 mmol), 1,3-dichloro-1,1,3,3-tetrabutyldistannoxane (0.30 mg, 0.05 mmol), and 2,6-di-tert-butyl-4-methylphenol (24 mg, 0.110 mmol) in dry THF (2 mL) were purged with nitrogen for 15 min at room temperature. The tube was sealed and stirred at 50 °C for 2 days. After cooling to room temperature, the reaction mixture was extracted using dichloromethane, and the extract was washed with water, dried over $Mg_2SO_4$, and then evaporated. The crude product was purified by column chromatography using dichloromethane as eluent and then washed with hexane. to yield yellow solid (0.84 g, 81%) $^1$H NMR (300 MHz, $CDCl_3$), $\delta$(ppm): 8.60 (d, $J$ = 5.7 Hz, 2H), 7.68 (d, $J$ = 7.8 Hz, 2H), 7.62–7.56 (m, 8H) 7.47–7.44 (m, 2H), 7.34–7.32 (m, 2H), 7.25 (d, $J$ = 2.7 Hz, 1H), 7.21 (d, $J$ = 2.7 Hz, 1H), 6.95 (d, $J$ = 8.7 Hz, 2H), 3.99 (t, $J$ = 6.6 Hz, 2H), 3.64 (t, $J$ = 6.6 Hz, 2H), 2.06–2.01 (m, 4H), 1.95 (s, 3H) 1.82–1.77 (m, 2H), 1.59–1.53 (m, 2H), 1.47–1.43 (m, 14H), 1.15–1.07 (m, 10H), 0.77–0.72 (m, 10H). MS (FAB): $m/z$ [$M^+$] 975; calcd $m/z$ [$M^+$] 974.46. Anal. Calcd for $C_{62}H_{71}NO_3S_3$: C, 76.42; H, 7.34; N, 1.44; Found: C, 76.49; H, 7.36; N, 1.92.

### 2.6. Synthesis of H-acceptor polymer

#### 2.6.1. Poly[10-(4-(5-(9,9-dihexyl-7-(5′-(pyridin-4-yl)-2,2′-bithiophen-5-yl)-9H-fluoren-2-yl)thiophen-2-yl)phenoxy)decyl methacrylate] (**PDFTP**)

The polymerization was carried out by the free radical polymerization described as follows. To a Schlenk tube, 1.5 g of monomer **DFTP** was dissolved in 20 wt% monomer concentration of dry THF (7.5 mL) with AIBN (5 mg, 2 mol % the monomer concentration) as an initiator. The solution was degassed by three freeze-pump-thaw cycles and then sealed off. The reaction mixture was stirred and heated at 60 °C for 48 h. After polymerization, the polymer was precipitated into methanol. The precipitated polymer was collected, washed with diethyl ether, and dried under high vacuum. Yield: 1.2 g (80%). $M_n = 25128$ and PDI ($M_w/M_n$) = 1.72 (by GPC). $^1$H NMR (300 MHz, $CDCl_3$), $\delta$(ppm): 8.51 (br, s, 2H), 7.55–7.46 (br, m, 4H), 7.32–7.11 (br, m, 10H), 6.95–6.91 (br, m, 2H), 6.81 (br, s, 2H), 3.99 (br, m, 2H), 3.83 (br, m, 2H), 1.95 (br, m, 4H), 1.72 (br, m, 4H), 1.33 (br, m, 12H), 0.98 (br, m, 12H), 0.64 (br, m, 10H). Anal. Calcd for $C_{62}H_{71}NO_3S_3$: C, 76.42; H, 7.34; N, 1.44; Found: C, 75.89; H, 7.11; N, 2.05.

#### 2.6.2. Preparation of H-Bonded polymer networks (**PDFTP/D1–D4**)

Proton-acceptor polymer **PDFTP** and proton-donor dye (**D1–D4**) 2:1 M ratio were dissolved in minimum amount of THF to make a clear solution. Then the solvent was evaporated under ambient temperature, and was followed by drying in a vacuum oven at 60 °C for several hours. The complexation of donor and acceptor through hydrogen bonding occurred during the solvent evaporation. Similar procedure was followed for all the H-bonded polymers.

## 3. Results and discussion

### 3.1. Structural characterization

All H-donor dyes **D1–D4**, monomer **DFTP**, and H-acceptor side-chain homopolymer **PDFTP** were satisfactorily characterized by $^1$H NMR, FAB, and elemental analyses. The weight average molecular weight (*M*w) of H-acceptor polymer **PDFTP** was determined by gel permeation chromatography (GPC) with THF as the eluting solvent and polystyrene as a standard. Fig. 3 shows $^1$H NMR spectra of monomer **DFTP** and polymer **PDFTP**. The number average molecular weight (*M*n) and polydispersity index (PDI) of polymer **PDFTP** were 25128 g/mol and 1.72, respectively. The decomposition temperatures ($T_d$) of H-bonded polymer networks **PDFTP/D1-D4** and H-acceptor polymer **PDFTP** were measured by TGA and summarized in Table 1. H-bonded cross-linking polymers showed good thermal stabilities with decomposition temperatures in the range of 381–386 °C, which are adequate for their applications in polymer solar cells and other optoelectronic devices.

**Table 1**
Photophysical Properties and Optical Band gaps of H-Donor Dyes (**D1–D4**), H-Acceptor Polymer (**PDFTP**), and H-Bonded Polymer Networks (**PDFTP/D1–D4**).

| Compound | $\lambda_{abs,sol}$ (nm)[a] | $\lambda_{abs,film}$ (nm)[a] | $\lambda_{onset,abs}$ (nm)[b] | $E_g^{opt}$ (eV)[b] | $T_d$ (°C) |
|---|---|---|---|---|---|
| **D1** | 470 | 513 | 646 | 1.91 | – |
| **D2** | 468 | 513 | 663 | 1.87 | – |
| **D3** | 480 | 530 | 639 | 1.94 | – |
| **D4** | 470 | 526 | 655 | 1.89 | – |
| **PDFTP** | 414 | 416 | 480 | 2.57 | – |
| **PDFTP/D1** | – | 426 | 586 | 2.11 | 381 |
| **PDFTP/D2** | – | 463 | 648 | 1.91 | 384 |
| **PDFTP/D3** | – | 445 | 604 | 2.05 | 386 |
| **PDFTP/D4** | – | 431 | 598 | 2.07 | 386 |

[a] Absorption spectra were recorded in THF solutions.
[b] Estimated from the onset wavelengths of absorption spectra in solid films.

### 3.2. FT-IR spectroscopy of H-Bonded cross-linking polymers

H-acceptor side-chain homopolymer **PDFTP** and H-donor dyes **D1–D4** were complexed in an appropriate molar ratio of 2:1 to form H-bonded cross-linking polymers by slow evaporation processes (ambient temperature) in THF solutions followed by drying under reduced pressure in vacuum. The formation of hydrogen bonds in H-bonded cross-linking polymers originated from COOH groups of H-donor dyes and pyridyl groups of H-acceptor polymer were confirmed by FTIR spectroscopy. Fig. 4 shows the IR spectra of H-donor dye **D1**, H-acceptor homopolymer **PDFTP**, and H-bonded polymer network **PDFTP/D1**. In contrast to the characteristic O–H stretching vibrations at 2490 and 2650 cm$^{-1}$ of pure **D1** dye, the weaker O–H bands observed at 2500 and 1900 cm$^{-1}$ are indicative of strong hydrogen bonding between the pyridyl groups of H-acceptor polymer **PDFTP** and carboxylic acids of H-donor **D1** dye [32,38]. In addition, the C=O stretching vibration at 1723 cm$^{-1}$ of H-bonded polymer network **PDFTP/D1** showed that the carbonyl group was in a less associated state than that in pure **D1** which appeared at 1678 cm$^{-1}$ [32b]. The above results implied that the hydrogen bonds were formed between H-acceptor polymer **PDFTP** and H-donor **D1** dye in the solid state of H-bonded polymer network **PDFTP/D1**. The other H-bonded cross-linking polymers also have the similar consequences as the H-bonded structure of H-bonded polymer network **PDFTP/D1** demonstrated here.

### 3.3. Optical properties

The normalized UV–vis absorption spectra of H-acceptor polymer **PDFTP** and H-donor dyes **D1–D4** in THF solutions ($10^{-5}$ M) are shown in Fig. 5 and their data are listed in Table 1. H-donor dyes **D1–D4** showed the maximum absorption wavelengths in the range from 468 to 480 nm and were attributed to the intramolecular charge transfer (ICT) from the donor carbazole core to the cyanoacrylic acid termini. Regardless of the increased conjugation lengths (with one more symmetrical thiophene unit) from **D1** to **D2**

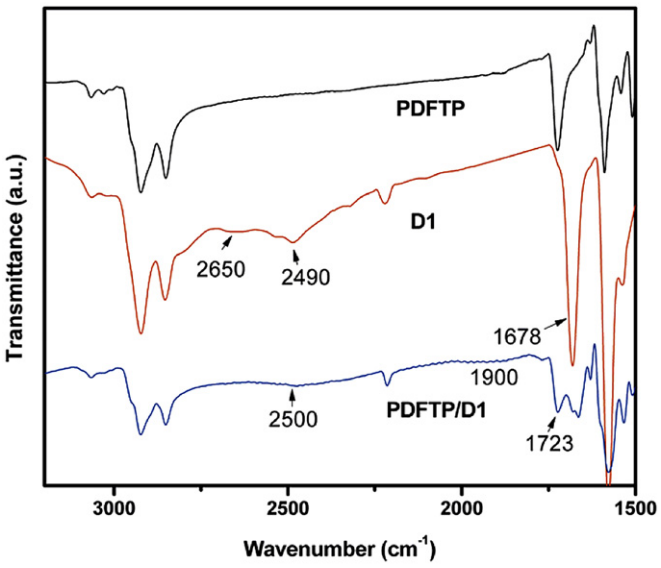


**Fig. 4.** FT-IR spectra of H-acceptor polymer **PDFTP**, H-donor dye **D1**, and H-bonded polymer network **PDFTP**/**D1** at room temperature.

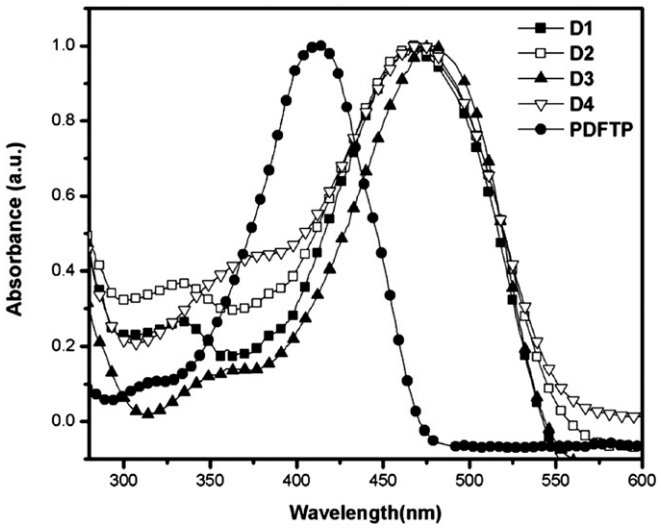


**Fig. 5.** Normalized UV–visible absorption spectra of H-donor dyes **D1**–**D4** and H-acceptor polymer **PDFTP** in THF solutions.

and from **D3** to **D4**, the presence of lateral alkyl chains in the thiophene units resulted in 2 and 10 nm blue shifts, respectively, which was presumably increased the disorder in the conjugated system of the dyes due to the steric hindrance imparted by those alkyl side chains. However, the onset absorption wavelengths were increased by the increased conjugation effect [39]. Relative to the solution state in Fig. 5, the solid film absorption spectra of dyes (**D1**–**D5**) in Fig. 6 a were red-shifted by a range of 43–56 nm (see Table 1), thus the red-shifts of the absorption peaks suggest the enhanced π-π stacking in terms of inter-chain characteristics [40] in solid state. As anticipated, the red-shifts from **D1** to **D3** (10 nm in solutions and 17 nm in solid films) and **D2** to **D4** (2 nm in solutions and 13 nm in solid films) were possible due to the enhanced π-π stacking assisted by the coplanar 2,7-carbazole cores of **D3** and **D4** over non-planar 3,6-carbazole cores of **D1** and **D2** [29e]. Evidently, the poor π-π stacking interactions in H-acceptor polymer **PDFTP**, due to presence of longer flexible alkyl chain resulted in negligible (2 nm) red shift in the absorption spectrum of solid film compared with that in solution. As shown in Fig. 6 b, the maximum absorption peak of H-bonded polymer networks **PDFTP/D1**–**D4** on solid quartz films were blue shifted in contrast to those of H-donor dyes (**D1**–**D4**) and the blue shifts (blue shifted to a range of 50–87 nm) were ascribed to the dilution effect of H-acceptor polymer as solid solvent for dyes as solutes in the H-bonded cross-linking polymers. However, the broader absorption spectra of H-bonded cross-linking polymers (compared with **PDFTP**) extending to longer wavelength regions (Fig. 6 b) favored better light harvesting and increased the photocurrent response region. In addition, the broadening of absorption spectra in the H-bonded cross-linking polymers increased their $\lambda_{onset}$, thus the decrease of optical band gaps in solid films was observed. Among all H-bonded polymer networks, **PDFTP/D2** has the longest broadening of the absorption spectrum. Thus, the lowest band gap (1.91 eV) of H-bonded polymer network **PDFTP/D2** was observed, which further reflected as the most superior performance among all photovoltaic devices. Furthermore, it is supported by the fact that there were significant PL quenching observed in the H-bonded polymer networks (see Fig. S1 of the supporting information) and the degrees of quenching were consistent with their PCE values (**PDFTP/D2** > **PDFTP/D1** > **PDFTP/D3** > **PDFTP/D4**). The largest PL quenching of **PDFTP/D2** was a symptom of better photo-induced charge transfer in H-bonded polymer network **PDFTP/D2**, which will reflect later to show the best PCE value.

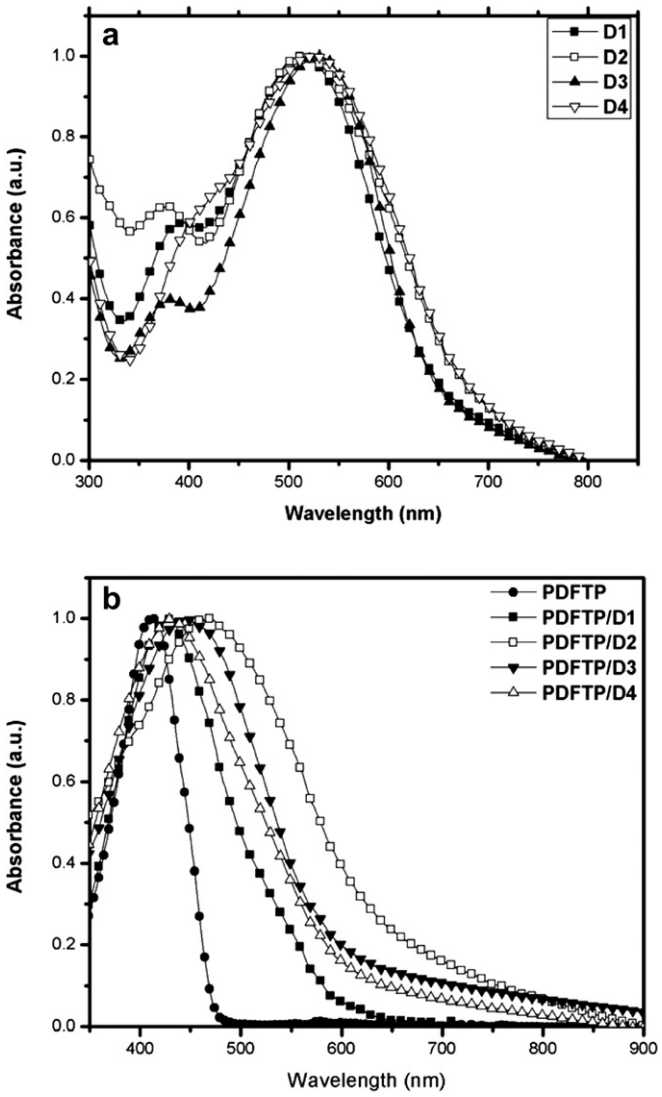


**Fig. 6.** Normalized UV–visible absorption spectra of (a) H-donor dyes (**D1**–**D4**) (b) H-acceptor polymer (**PDFTP**) and H-bonded polymer networks (**PDFTP/D1**–**D4**) in solid films coated onto fused quartz plates.

### 3.4. Electrochemical properties

Cyclic voltammetric (CV) method was used to investigate the electrochemical characteristics of H-donor dyes (**D1**–**D4**), H-acceptor polymer **PDFTP**, and the H-bonded polymer networks (**PDFTP/D1**–**D4**). The relevant CV data of dyes are presented in

**Table 2**
Electrochemical Properties of H-Acceptor Polymer (**PDFTP**) and H-Bonded Polymer Networks (**PDFTP/D1**–**D4**).

| Polymer | $E_{ox/onset}$ (V)[a] | $E_{red/onset}$ (V)[a] | HOMO (eV)[b] | LUMO (eV)[b] | $E_{g,cv}$ (eV)[c] |
|---|---|---|---|---|---|
| **PDFTP** | 1.28 | − 0.90 | − 5.63 | − 3.45 | 2.21 |
| **PDFTP/D1** | 1.16 | − 0.94 | − 5.51 | − 3.41 | 2.10 |
| **PDFTP/D2** | 1.02 | − 0.83 | − 5.37 | − 3.52 | 1.85 |
| **PDFTP/D3** | 1.06 | − 0.96 | − 5.41 | − 3.39 | 2.02 |
| **PDFTP/D4** | 1.14 | − 0.83 | − 5.49 | − 3.52 | 1.97 |

[a] Oxidation and reduction potentials were measured by cyclic voltammetry in solid films.
[b] Estimated from the onset potentials using empirical equations: HOMO/LUMO = $[-(E_{ox/red\ onset} - E_{1/2\ (ferrocene)} + 4.8)]$ eV, where 4.8 eV is the energy level of ferrocene below the vacuum level.
[c] Band gaps measured by cyclic voltammograms.

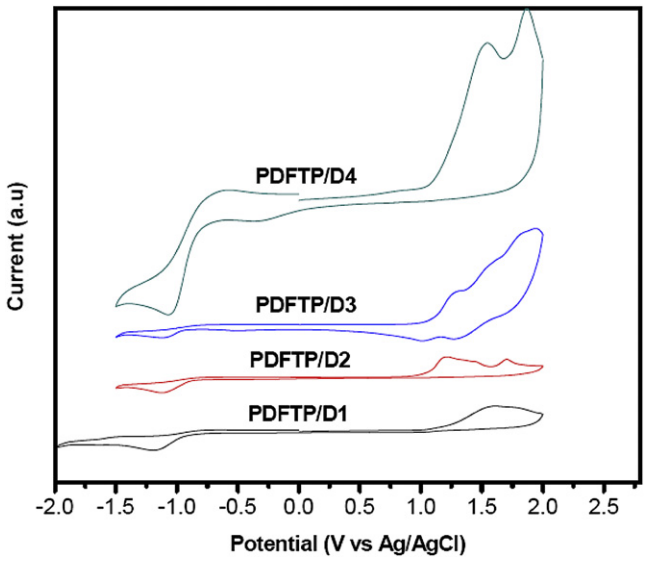


**Fig. 7.** Cyclic voltammograms of H-bonded polymer networks **PDFTP/D1–D4** in acetonitrile at a scan rate of 100 mV/s.

Table S1 and Fig. S2 (see the supporting information), and those of polymers are also illustrated in Table 2 and Fig. 7. Cyclic voltammograms of the dyes are measured in deoxygenated THF solutions containing 0.1 M $TBAPF_6$ at 25 °C in volts versus $Ag/AgNO_3$ (0.01 M in MeCN; the scan rate is 100 mV $s^{-1}$). All dyes (**D1–D4**) exhibited quasi-reversible oxidation and reduction potential (see Fig. S2 of the supporting information). The calculated HOMO and LUMO levels of those H-donor dyes **D1–D4** were found in the range of − 5.44 to − 5.56 eV and − 3.31 to − 3.34 eV, respectively, with electrochemical band gap of 2.11–2.22 eV. Cyclic voltammograms of H-acceptor polymer **PDFTP** and H-bonded polymer networks **PDFTP/D1–D4** were measured in solid films with Ag/AgCl as a reference electrode, which were calibrated by ferrocene ($E_{1/2\,(ferrocene)}$ = 0.45 mV vs Ag/AgCl). The HOMO and LUMO levels of all polymers were estimated by the oxidation and reduction potentials from the reference energy level of ferrocene (4.8 eV below the vacuum level) according to the following equation [41]: $E_{HOMO/LUMO}$ = [-($E_{onset}$ - 0.45) - 4.8] eV. The HOMO/LUMO levels of H-bonded polymer networks **PDFTP/D1–D4** were estimated to be − 5.51/− 3.41, − 5.37/− 3.52, − 5.41/− 3.39, and − 5.49/− 3.52 eV, respectively, with electrochemical band gaps ($E_{g,cv}$) of 2.10, 1.85, 2.02, and 1.97 eV, correspondingly. The attained LUMO and HOMO levels in these H-bonded polymer networks with good air stabilities are suitable as a donor for electron injection and transporting to PCBM acceptor [42]. Moreover, electrochemical band gaps ($E_{g,cv}$) were very close to those obtained from the absorption spectra of solid polymer films ($E_{g,opt}$). To gain insight into the geometries of H-donor dyes **D1–D4**, we performed DFT (density functional theory) calculations using Gaussian 03 program package. The optimized geometries in ground state and the dihedral angles formed between the carbazole-thiophene and thiophene-cyanoacrylate units are shown in Fig. S3 and Table S2 of the supporting information. From the calculated dihedral angles, it is noticeable that the thiophene units are found to be coplanar with the cyanoacrylic acid groups, which are important characteristics in the conceptions of materials in photovoltaic applications.

**Table 3**
Photovoltaic Performance of PSC Devices[a] Based on H-Bonded Polymer Networks **PDFTP/D1-D4** Measured Under AM 1.5 Irradiation, 100 mW/$cm^2$.

| Polymer network | $V_{oc}$ (V) | $J_{sc}$ (mA/$cm^2$) | FF (%) | PCE (%) |
|---|---|---|---|---|
| **PDFTP/D1** | 0.56 | 1.76 | 27 | 0.27 |
| **PDFTP/D2** | 0.55 | 1.90 | 29 | 0.31 |
| **PDFTP/D3** | 0.57 | 1.40 | 30 | 0.24 |
| **PDFTP/D4** | 0.59 | 1.13 | 24 | 0.16 |

[a] PSC devices with the configuration of ITO/PEDOT:PSS/(**PDFTP/D1-D4**):PCBM/Ca/Al where H-bonded polymer network:PCBM = 1:1 by weight.

### 3.5. Photovoltaic properties

To demonstrate the potential application of the H-bonded polymer networks (**PDFTP/D1–D4**) as electron donors in photovoltaic devices, we fabricated devices by spin-coating from 2 wt% N-methylpyrrolidone (NMP) solutions of polymer blends containing H-bonded polymer networks **PDFTP/D1–D4** (as electron donors) and PCBM (as an electron acceptor) in 1:1 weight ratio with a configuration of ITO/PEDOT:PSS/H-bonded polymer networks:PCBM (1:1 w/w)/Ca/Al (under AM 1.5 irradiation, 100 mW/$cm^2$). Fig. 8 shows the current density versus voltage ($J$–$V$) curves and the results are illustrated in Table 3. As shown in Table 3, the short-circuit current density ($J_{sc}$), open-circuit voltage ($V_{oc}$), fill factor (FF), and PCE values of the OPV devices containing H-bonded

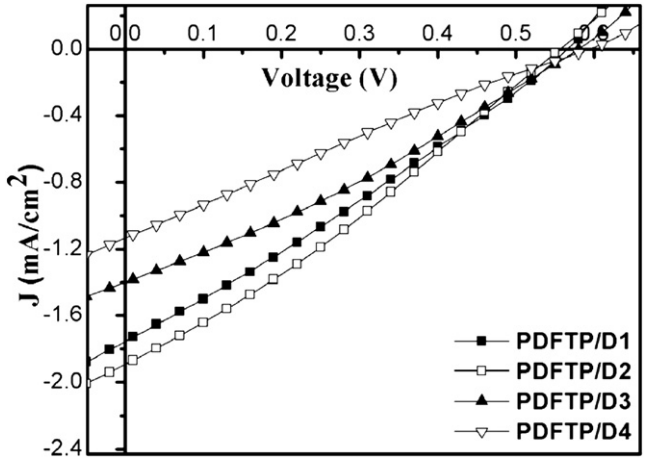


**Fig. 8.** Current density-voltage curves of illuminated solar cells incorporating H-bonded polymer networks **PDFTP/D1–D4** with PCBM in 1:1 (w/w) ratio under AM 1.5G, 100 mW/$cm^2$.

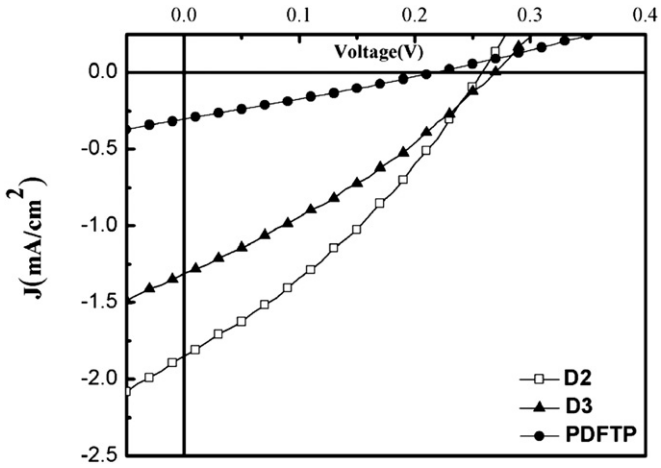


**Fig. 9.** Current density-voltage curves of illuminated solar cells incorporating **D2**, **D3**, or **PDFTP** with PCBM in 1:1 (w/w) ratio under AM 1.5G, 100 mW/$cm^2$.

**Table 4**
Photovoltaic Performance of PSC Devices[a] Based on H-Donor Dyes **D2-D3** or H-Acceptor Polymer **PDFTP** Measured Under AM 1.5 Irradiation, 100 mW/cm$^2$.

| Compound | $V_{oc}$ (V) | $J_{sc}$ (mA/cm$^2$) | FF (%) | PCE (%) |
|---|---|---|---|---|
| **D2** | 0.26 | 1.85 | 32 | 0.15 |
| **D3** | 0.27 | 1.31 | 31 | 0.11 |
| **PDFTP** | 0.22 | 0.30 | 26 | 0.02 |

[a] PSC devices with the configuration of ITO/PEDOT:PSS/**D2,D3**, or **PDFTP**:PCBM/Ca/Al where Compound:PCBM = 1:1 by weight.

polymer networks **PDFTP/D1**–**D4** were in the range of 1.13–1.9 mA/cm$^2$, 0.55–0.59 V, 24–30%, 0.16–0.31%, respectively. Due to the negligible difference in their HOMO values, all the devices containing H-bonded polymer networks (**PDFTP/D1**–**D4**) showed similar $V_{oc}$ values. As described before, due to the longest broadening of absorption spectra in **PDFTP/D2**, it had the best light harvesting and the highest photocurrent response and hence to appeal a highest $J_{sc}$ value (1.9 mA/cm$^2$) among all H-bonded polymer networks (**PDFTP/D1**–**D4**). As a contributing parameter for the net PCE value, the fill factors of the OPV devices were low, which could be associated with the large series resistance of the devices. In addition, the behavior of the solar cell properties can be well analyzed from the surface topography of the active layer. On the whole, the OPV device containing blended H-bonded polymer network **PDFTP/D2**:PCBM resulted the best overall PCE value of 0.31% with $J_{sc}$ = 1.9 mA/cm$^2$, $V_{oc}$ = 0.55 V, and FF = 29%, which was mainly because of its broader absorption and better utilization of the solar spectrum, and also supported by the largest quenching of PL spectra (see Fig. S1 of the supporting information) which increased the photo-induced charge transfer in H-bonded polymer network **PDFTP/D2** [14b,19c]. In general, the poor solubilities of H-bonded polymer networks might be one of the reasons for the lower PCE values. In order to demonstrate the contribution of supramolecular structures in H-bonded cross-linking polymers, we fabricated OPV devices with only H-donor **D2**–**D3** dyes or H-acceptor polymer **PDFTP** blended with PCBM in 1:1 weight ratio measured under similar conditions as those of the blended H-bonded cross-linking polymers and the *J-V* curves are shown in Fig. 9 and the data are listed in Table 4. Interestingly, it is noticeable that the PCE values of **D2** (0.15%), **D3** (0.11%), and **PDFTP** (0.02%) were much lower than those of H-bonded polymer networks **PDFTP/D2** (0.31%) and P**DFTP/D3** (0.24%). In general, the approach in self-assembly of H-donor dyes with H-acceptor polymers via hydrogen bonding was proven to enhance OPV properties by the unique non-covalent-bonded practical applications.

## 4. Conclusions

In order to get the advantage from physical properties of both small molecules and polymers in OPV devices, the concept of supramolecular architectures by complexation of H-donor dyes (**D1**–**D4**) with a side-chain H-acceptor homopolymer (**PDFTP**) was applied to produce H-bonded cross-linking polymers. Photophysical properties revealed that the absorption spectra of H-bonded polymer networks showed broader wavelength ranges and higher $\lambda_{onset}$ values to appeal better light harvesting, though they showed blue shifts in their respective absorption maxima ($\lambda_{max}$). The H-bonded polymer networks (**PDFTP/D1**–**D4**) had much higher PCE values than the individual H-donor dyes (**D1**–**D4**) or H-acceptor polymer (**PDFTP**). The H-bonded polymer network **PDFTP/D2** containing **D2** dye showed the best photovoltaic performance with a PCE value of 0.31%, which is double of the PCE value (0.15%) in the corresponding **D2** dye, fabricated and measured under similar conditions. Thus, the results by complexation of small molecules and polymers via H-bonding are very encouraging for the future research on donor-acceptor supramolecular architectures of oligomeric dyes H-bonded with processable π-conjugated polymers in organic solar cell applications.

## Appendix. Supplementary material

Supplementary data related to this article can be found online at doi:10.1016/j.polymer.2010.10.018.

## References


[1] Gonçalves LM, Bermudez VDZ, Ribeiroa HA, Mendes AM. Energy Environ Sci 2008;1:655–67.
[2] Kaygusuz K. Energy Sources 2002;24:787–99.
[3] (a) Lewis NS. Science 2007;315:798–801;
(b) Scharber CM, Mühlbacher D, Koppe M, Denk P, Waldauf C, Heeger AJ, et al. Adv Mater 2006;16:789–94.
[4] (a) Burroughs JH, Bradley DDC, Brown AR, Marks RN, Mackay K, Friend RH, et al. Nature 1990;347:539–41;
(b) Gustafasson G, Cao Y, Treacy GM, Klavetter F, Colaneri N, Heeger AJ. Nature 1992;357:477–9.
[5] (a) Sariciftci NS, Smilowitz L, Heeger AJ. Science 1992;258:1474–6;
(b) Zhang S, Guo Y, Fan H, Liu Y, Chen H-Y, Yang G, et al. J Polym Sci Part A Polym Chem 2009;47:5498–508.
[6] (a) Xue L, He J, Gu X, Yang Z, Xu B, Tian W. J Phys Chem C 2009;113:12911–7;
(b) Chen CP, Chan SH, Chao TC, Ting C, Ko BT. J Am Chem Soc 2008;130:12828–33;
(c) Huo L, Hou J, Zhang S, Chen HY, Yang Y. Angew Chem Int Ed 2010;49:1500–3;
(d) Tang W, Kietzke T, Vemulamada P, Chen ZK. J Polym Sci Part A Polym Chem 2007;45:5266–76.
[7] (a) Yu G, Gao J, Hummelen JC, Wudl F, Heeger AJ. Science 1995;270:1789–91;
(b) Hou J, Chen TL, Zhang S, Huo L, Sista S, Yang Y. Macromolecules 2009;42:9217–9.
[8] (a) Gunes S, Neugebauer H, Sariciftci NS. Chem Rev 2007;107:1324–38;
(b) Tamayo AB, Dang XD, Walker B, Seo J, Kent T, Nguyen TQ. Appl Phys Lett 2009;94:103301.
[9] Thompson BC, Frechet JMJ. Angew Chem Int Ed 2008;47:58–77.
[10] (a) O'Regan B, Grätzel M. Nature 1991;353:737–40;
(b) Grätzel M. Nature 2001;414:338–44.
[11] (a) Mishra A, Fischer MKR, Bäuerle P. Angew Chem Int Ed 2009;48:2474–99;
(b) Yen YS, Hsu YC, Lin JT, Chang CW, Hsu CP, Yin DJ. J Phys Chem C 2008;112:12557–67.
[12] (a) Huang ST, Hsu YC, Yen YS, Chou HH, Lin JT, Chang CW, et al. Phys Chem C 2008;112:19739–47;
(b) Koumura N, Wang ZS, Miyashita M, Uemura Y, Sekiguchi H, Cui Y, Mori A, et al. J Mater Chem 2009;19:4829–36.
[13] (a) Tang CW. Appl Phys Lett 1986;48:183–5;
(b) Chen GY, Chiang CM, Kekuda D, Lan SC, Chu CW, Wei KW. J Polym Sci Part A Polym Chem 2010;48:1669–75.
[14] (a) Chang YT, Hsu SL, Su MH, Wei KH. Adv Mater 2009;21:1–5;
(b) Li Y, Li Z, Wang C, Li H, Lu H, Xu B, et al. J Polym Sci Part A Polym Chem 2010;48:2765–76;
(c) Li Y, Li H, Xu B, Li Z, Chen F, Feng D, et al. Polymer 2010;51:1786–95.
[15] Peumans P, Uchida S, Forrest SR. Nature 2003;425:158–62.
[16] (a) Uchida S, Xue J, Rand BP, Forrest SR. Appl Phys Lett 2004;84:4218–20;
(b) Sharma GD, Balraju P, Mikroyannidis JA, Stylianakis MM. Sol Energy Mater Sol Cells 2009;93:2025–8.
[17] Granstrom M, Petritsch K, Arias AC, Lux A, Andersson MR, Friend RH. Nature 1998;395:257–60.
[18] Halls JJM, Walsh CA, Greenham NC, Marseglia EA, Friend RH, Moratti SC, et al. Nature 1995;376:498–500.
[19] (a) Zhou E, Wei Q, Yamakawa S, Zhang Y, Tajima K, Yang C, et al. Macromolecules 2010;21:821–6;
(b) Zhang S, He C, Liu Y, Zhan X, Chen J. Polymer 2009;50:3595–9;
(c) Chang YT, Hsu SL, Su MH, Wei KH. Adv Funct Mater 2007;17:3326–31.
[20] Lindner SM, Hüttner S, Chiche A, Thelakkat M, Krausch G. Angew Chem Int Ed 2006;45:3364–8.
[21] (a) Silvestri F, Duarte IL, Seitz W, Beverina L, Díaz MVM, Marks TJ, et al. Chem Commun; 2009:4500–2;
(b) Huang CH, McClenaghan ND, Kuhn A, Bravic G, Bassani DM. Tetrahedron 2006;62:2050–9;
(c) Sánchez L, Sierra M, Martín N, Myles AJ, Dale Jr TJ, Seitz W, et al. Angew Chem Int Ed 2006;45:4637–41;
(d) Roncali J. Chem Soc Rev 2005;34:483–95.
[22] (a) Jonkheijm P, Duren JKJV, Kemerink M, Janssen RAJ, Schenning APHJ, Meijer EW. Macromolecules 2006;39:784–8;
(b) Schmidt-Mende L, Fechtenkötter A, Müllen K, Moons E, Friend RH, MacKenzie JD. Science 2001;293:1119–22.

[23] (a) Würthner F, Chen Z, Hoeben FJM, Peter Osswald P, You CC, Jonkheijm P, et al. J Am Chem Soc 2004;126:10611–8;
(b) Herrikhuyzen JV, Syamakumari A, Schenning APHJ, Meijer EW. J Am Chem Soc 2004;126:10021–7;
(c) Huang CH, McClenaghan ND, Kuhn A, Hofstraat JW, Bassani DM. Org Lett 2005;7:3409–12;
(d) Chu CC, Bassani DM. Photochem Photobiol Sci 2008;7:521–30.
[24] (a) Kim J, Park SH, Cho S, Jin Y, Kim J, Kim I, et al. Polymer 2010;51:390–6;
(b) Zhang G, Fu Y, Zhang Q, Xie Z. Polymer 2010;51:2313–9;
(c) Cho S, Seo JH, Kim SH, Song S, Jin Y, Lee K, et al. Appl Phys Lett 2008;93:263301;
(d) Kim J, Kim SH, Jung IH, Jeong E, Xia Y, Cho, Hwang IW, et al. J Mate Chem 2010;20:1577–86.
[25] (a) Jin Y, Kim JY, Park SH, Kim J, Lee S, Lee K, et al. Polymer 2005;46:12158–65;
(b) Song S, Jin Y, Kim SH, Shim JY, Son S, Kim I, et al. J Polym Sci Part A Polym Chem 2009;47:6540–51;
(c) Lee TH, Lai KM, Leung LM. Polymer 2009;50:4602–11;
(d) Wu CW, Tsai CM, Lin HC. Macromolecules 2006;39:4298–305;
(e) Lee KW, Lin HC. Polymer 2007;48:3664–72.
[26] (a) Jérome D, Bechgaard K. Nature 2001;410:162–3;
(b) Yoon H, Lee SH, Kwon OS, Song HS, Oh EH, Park TH, et al. Angew Chem Int Ed 2009;48:2755–8;
(c) Kim DH, Park YD, Jang Y, Yang H, Kim YH, Han JI, et al. Adv Funct Mater 2005;15:77–82.
[27] (a) TamayoAB WalkerB, Nguyen TQ. J Phys Chem 2008;112:11545–51;
(b) Li KC, Huang JH, Hsu YC, Huang PJ, Chu CW, Lin JT, et al. Macromolecules 2009;42:3681–93.
[28] Morin JF, Leclerc M. Macromolecules 2001;34:4680–2.
[29] (a) Freeman AW, Urvoy M, Criswell ME. J Org Chem 2005;70:5014–9;
(b) Blouin N, Michaud A, Leclerc M. Adv Mater 2007;19:2295–300;
(c) Tomkeviciene A, Grazulevicius JV, Jankauskas V. Chem Lett 2008;37:344–5;
(d) Blouin N, Michaud A, Gendron D, Wakim S, Blair E, Neagu-Plesu R, et al. J Am Chem Soc 2008;130:732–42;
(e) Wang HL, Wang XY, Wang L, Wang HL, Liu AH. Chin J Struct Chem; 2007:413–8.
[30] (a) Wakim S, Beaupré S, Blouin N, Aich BR, Rodman S, Gaudiana R, et al. J Mater Chem 2009;19:5351–8;
(b) Ooi ZE, Tam TL, Shin RYC, Chen ZK, Kietzke T, Sellinger A, et al. J Mater Chem 2008;18:4619–22;
(c) Blouin N, Leclerc M. Acc Chem Res 2008;41:1110–9;
(d) Yuan MC, Su MH, Chiu MY, Wei KH. J Polym Sci Part A Polym Chem 2010;48:1298–309.
[31] (a) Fukuzumi S, Honda T, Ohkubo K, Kojima T. Dalton Trans; 2009:3880–9;
(b) El-ghayoury A, Schenning APHJ, Hal PAV, Duren JKJV, Janssen RAJ, Meijer EW. Angew Chem Int Ed 2001;40:3660–3.
[32] (a) Yang PJ, Wu CW, Sahu D, Lin HC. Macromolecules 2008;41:9692–703;
(b) Liang TC, Chiang IH, Yang PJ, Kekuda D, Chu CW, Lin HC. J Polym Sci Part A Polym Chem 2009;47:5998–6013.
[33] (a) Becke AD. J Chem Phys 1993;98:5648–52;
(b) Lee C, Yang W, Par RG. Phys Rev B 1988;37:785–9.
[34] (a) Hey PJ, Wadt WR. J Chem Phys 1985;82:270–83;
(b) Wadt WR, Hey PJ. J Chem Phys 1985;82:284–98.
[35] Pople JA. Gaussian 03, revision E.01. Wallingford, CT: Gaussian, Inc.; 2004.
[36] Wang Y, Hou L, Yang K, Chen J, Wang F, Cao Y. Macromol Chem Phys 2005;206:2190–8.
[37] Blouin N, Michaud A, Leclerc M. Adv Mater 2007;19:2295–300.
[38] Lee JY, Painter PC, Coleman MM. Macromolecules 1988;21:954–60.
[39] (a) Wang ZS, Koumura N, Cui Y, Takahashi M, Sekugichi H, Mori A, et al. Chem Mater 2008;20:3993–4003;
(b) Kim D, Lee JK, Kang SO, Ko J. Tetrahedron 2007;63:1913–22;
(c) Yue W, Zhao Y, Shao S, Tian H, Xie Z, Geng Y, et al. J Mater Chem 2009;19:2199–206.
[40] Hau J, Fan B, Huo L, He C, Yang C, Li YF. J Polym Sci Part A Polym Chem 2006;44:1279–90.
[41] Li KC, Hsu YC, Lin JT, Yang CC, Wei KH, Lin HC. J Polym Sci Part A Polym Chem 2009;47:2073–92.
[42] de Leeuw DM, Simenon MMJ, Brown AR, Einhard REF. Synth Met 1997;87:53–9.